The magnetic phases of pseudobinary $Ce(Fe_{1-x}M_x)_2$ intermetallic compounds; M=Al, Co, Ru

1990 J. Phys.: Condens. Matter 2 1213

(http://iopscience.iop.org/0953-8984/2/5/013)

J. Phys.: Condens. Matter **2** (1990) 1213–1222. Printed in the UK

The magnetic phases of pseudobinary $Ce(Fe_{1-x}M_x)_2$ intermetallic compounds; M = Al, Co, Ru

S J Kennedy† and B R Coles
Blackett Laboratory, Imperial College, London SW7 2BZ, UK

Received 27 July 1989

Abstract. Powder neutron diffraction measurements of the magnetic and structural properties of a range of pseudobinary $Ce(Fe_{1-x}M_x)_2$ intermetallic compounds, with M = Al, Co, Ru, are reported.

In each of these pseudobinaries addition of a small amount of the metallic impurity (M) to $CeFe_2$ reduces the ferromagnetic ordering temperature and enhances the small antiferromagnetic component which appears at low temperature. At higher impurity concentrations antiferromagnetism is achieved. This antiferromagnetism is accompanied by a cubic to rhombohedral distortion of the crystalline lattice.

The antiferromagnetic component of the ordered moment in these compounds is oriented at $\simeq 18.5°$ to the antiferromagnetic propagation vector ($\tau = \langle 111 \rangle$). An ordered cerium moment is seen in the ferromagnetic phase of $CeFe_2$ and $Ce(Fe_{1-x}Ru_x)_2$. This moment is coupled ferrimagnetically to the iron-sublattice moment and $\vec{\mu}_{Ce}/\vec{\mu}_{Fe} \simeq -0.3$.

1. Introduction

Investigation of the anomalous magnetic properties of the ferromagnetic cubic Laves phase compound $CeFe_2$ is currently attracting renewed interest since the discovery that addition of metallic impurities such as Al (Franceschini and Da Cunha 1985) and Co (Rastogi and Murani 1987) to the Fe sites destabilises ferromagnetism causing in some cases a total loss of ferromagnetism. Subsequently bulk magnetic properties of several other $Ce(Fe_{1-x}M_x)_2$ pseudobinaries with M = Ru, Si, Os, Ir (Roy and Coles 1987, Tandon *et al* 1989, Roy *et al* 1988) have shown similar magnetic instabilities. Whereas substitutions of M = Ni, Cu, Rh, Mn onto the Fe sites have shown no such instability (Rastogi and Murani 1987, Tandon *et al* 1989, Roy and Coles 1989). Although Ce has been thought to be non-magnetic in $CeFe_2$, the role of hybridisation of the 4f orbital and 3d band electrons has been suggested as an important factor in the magnetic behaviour of $CeFe_2$ (Eriksson *et al* 1988), and indeed substitution of Y and U onto the Ce sites in the anomalous pseudobinaries has resulted in a return to normal magnetic behaviour (Tandon *et al* 1989, Roy and Coles 1989).

Speculation as to the magnetic order of the non-ferromagnetic phase of the anomalous pseudobinaries has included suggestions of antiferromagnetic, spin-canted and reentrant spin glass phases. Our earlier neutron diffraction measurements on $Ce(Fe_{1-x}Co_x)_2$ showed that ferromagnetic order of the Fe atoms is replaced by anti-

† Now at; AINSE, Building 58, Private Mail Bag No 1, Menai 2234, New South Wales, Australia.

0953-8984/90/051213 + 10 $03.50

ferromagnetism at low temperature and allowed us to identify the magnetic structure of this phase (Kennedy *et al* 1989). High resolution neutron powder diffraction enabled identification of a rhombohedral distortion of the cubic lattice in the antiferromagnetic phase (Kennedy *et al* 1988) and also showed that this distortion coincides with the onset of antiferromagnetism.

In this report we have extended our powder neutron diffraction measurements to include investigation of the magnetic phases of pseudobinaries with M = Al, Ru and also the parent compound $CeFe_2$. We have also performed more detailed analysis of the diffraction data to assess the possibility of contributions from the Ce sites to long range magnetic order.

2. Experimental details

The pseudobinary $Ce(Fe_{1-x}M_x)_2$ intermetallic compounds under investigation were prepared as previously described (Roy and Coles 1987, Kennedy *et al* 1988) using 99.99% pure or better Ce, Co, Fe, Al, Ru. The method of preparation involves multiple melting of constituent elements into buttons in an argon arc furnace followed by annealing *in vacuo* in three stages at 600 °C, 700 °C and 800 °C over seven days. The compounds were ground into fine powders with mortar and pestle under argon atmosphere. The compounds were $CeFe_2$, $Ce(Fe_{1-x}Al_x)_2$ with $x = 0.02, 0.035, 0.08$, $Ce(Fe_{0.80}Co_{0.20})_2$ and $Ce(Fe_{1-x}Ru_x)_2$ with $x = 0.02, 0.04, 0.06$. Powdered samples were 25 to 30 g in weight and neutron diffraction measurements showed impurity (Ce_2Fe_{17}) concentrations to be $<0.5\%$.

Structural measuements have been performed on the $CeFe_2$, $Ce(Fe_{1-x}Co_x)_2$ and $Ce(Fe_{1-x}Ru_x)_2$ compounds in the temperature range 5 K to 300 K on the high resolution neutron powder diffractometer HRPD at ISIS—the Rutherford Appleton Laboratory spallation neutron source (Johnson and David 1985). Magnetic measurements were performed on all compounds in the temperature range 5 K to 300 K in steps of $\simeq 2$ K, at a wavelength of 2.52 Å on the high intensity neutron powder diffractometer D1B at Institut Laue-Langevin, Grenoble. For the purpose of analysis the D1B diffraction patterns were summed over $\simeq \pm 8$ K.

The magnetic and structural results of the $Ce(Fe_{1-x}Co_x)_2$ compounds are as reported previously (Kennedy *et al* 1987, 1988), but a reanalysis of the magnetic information is presented here which includes the full magnetic structure factor and a more complete analysis of the temperature dependence of the magnetic components.

3. Results and analysis

3.1. Structural results

The high resolution diffraction patterns on HRPD from $CeFe_2$ and the $Ce(Fe_{1-x}Ru_x)_2$ compounds were analysed using the Reitveld structural refinement method to extract the structural parameters. These refinements gave an upper limit of $\simeq 1\%$ occupancy of Ce sites by transition metal atoms, and the substitution of the M atoms at the Fe sites appears to be random within a few per cent. $CeFe_2$ and $Ce(Fe_{0.98}Ru_{0.02})_2$ were found to be cubic at 5 K (space group $Fd\bar{3}m$). $Ce(Fe_{0.96}Ru_{0.04})_2$ was found to undergo a rhombohedral distortion at T_N ($\simeq 80$ K) and refined with space group $R\bar{3}m$ below this

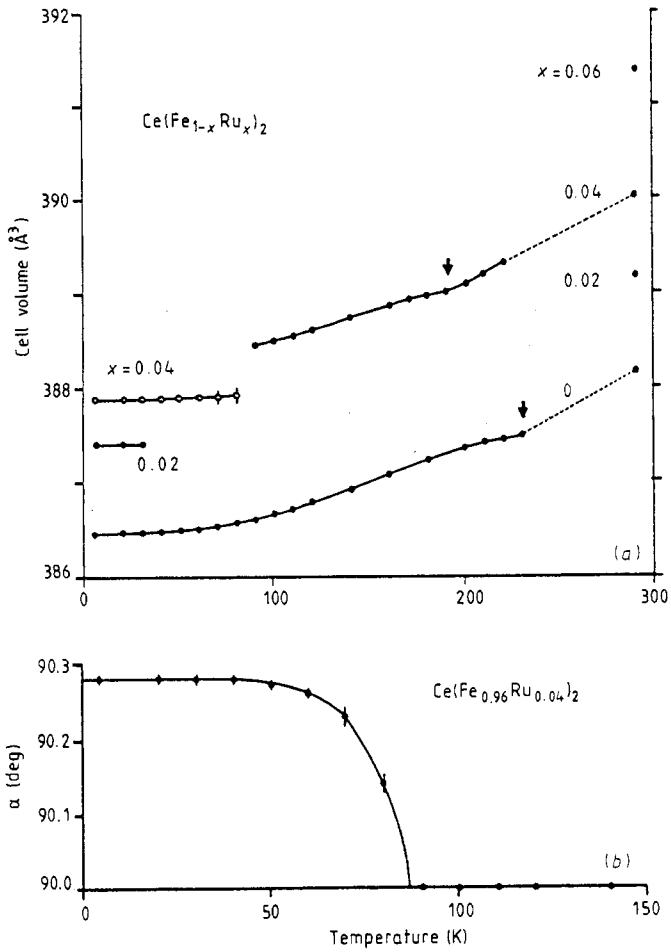

Figure 1. (*a*) Temperature and concentration dependences of lattice cell volume for $Ce(Fe_{1-x}Ru_x)_2$ compounds with $x = 0.00, 0.02, 0.04, 0.06$, showing the cubic to rhombohedral distortion at T_N in $Ce(Fe_{0.96}Ru_{0.04})_2$. Open circles indicate space group $R\bar{3}m$, closed circles indicate space group $Fd\bar{3}m$. T_c for $x = 0.00, 0.04$ indicated by arrows. (*b*) Temperature dependence of cell-axis angle (α) for $Ce(Fe_{0.96}Ru_{0.04})_2$.

temperature, as found previously in $Ce(Fe_{1-x}Co_x)_2$ ($x = 0.15, 0.20$). $Ce(Fe_{0.94}Ru_{0.06})_2$ was found to be cubic at room temperature ($Fd\bar{3}m$). The $Ce(Fe_{1-x}Al_x)_2$ compounds were not measured on HRPD, but D1B results indicate that these pseudo-binaries, and the $Ce(Fe_{0.94}Ru_{0.06})_2$ compound, also undergo a rhombohedral lattice distortion at or around T_N. The extent of the rhombohedral distortion, as measured on D1B, was calculated from the temperature dependence of the measured peak width of the (220) nuclear reflection, which undergoes two-fold splitting under cubic-rhombohedral distortion. Although this splitting is unresolved on D1B the results yield lattice cell angles (α's) which are in agreement with the HRPD results where the latter have been determined.

The results of the HRPD refinements are presented in figure 1(*a*), which shows the temperature and concentration dependence of cell volume for $Ce(Fe_{1-x}Ru_x)_2$ with $x =$

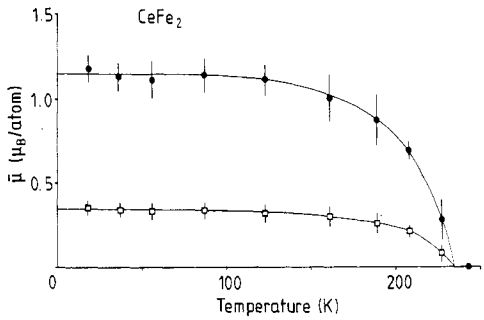

Figure 2. Temperature dependence of the ordered magnetic moment contributions in $CeFe_2$. Ferromagnetic Fe-site moment (●), ferromagnetic Ce-site moment (□). Note that these moments are ferrimagnetically coupled, and that there is a small antiferromagnetic component below 60 K (not shown on figure).

0.00, 0.02, 0.04, 0.06, and figure 1(*b*), which shows the temperature dependence of the lattice distortion ($\propto$) for $x = 0.04$. The temperature dependence of the lattice distortions ($\propto -90°$) are indicated by crosses where appropriate (and drawn to scale) in the plots of the D1B results (figures 2–5).

3.2. *Magnetic analysis*

3.2.1. Ferromagnetic Bragg scattering. The observed D1B diffraction patterns were fitted to Gaussian lineshapes and the nuclear Bragg scattering intensities used to calibrate the magnetic Bragg scattering intensities. The observed nuclear Bragg reflections on D1B; (111), (311) and (220) all show significant ferromagnetic contributions below T_c when the Debye Waller temperature corrections are applied, and in addition the (220) nuclear reflection shows a ferromagnetic contribution in $Ce(Fe_{1-x}Ru_x)_2$, $x = 0.00, 0.02, 0.06$. The ferromagnetic Bragg scattering intensity for a polycrystalline, cylindrical specimen is given by

$$I_f \propto \left(\frac{e^2\gamma^2}{2mc^2}\right) \frac{j\bar{q}^2[F(hkl)]^2 \exp(-2W)}{\sin\theta_B \sin 2\theta_B}$$

where I_f is the integrated intensity, j is the multiplicity of the reflection, $\bar{q}^2$ is the average spin orientation factor ($=2/3$ for a ferromagnet), $\sin\theta_B \sin 2\theta_B$ is the Lorentz factor and $\exp(-2W)$ is the Debye–Waller factor.

The Debye–Waller factor was calculated using a second-order expansion of the approximation of Lovesey (1986). The ferromagnetic structure factors ($F(hkl)$) for the observed reflections of $CeFe_2$ are presented in table 1, where we see that the (111) and (311) reflections have contributions from both the Ce and Fe sublattices, the (220) reflection is due solely to Ce moments and the (222) reflection is due solely to Fe moments.

Here f and $\bar{\mu}$ are the magnetic form factor and average magnetic moment, respectively. The calculated magnetic form factor for Fe was taken from the calculations of Freeman and Watson (1961) for 3d electrons, and the Ce magnetic moments were assumed to possess a Ce^{3+} (4f electron) magnetic form factor (Stassis *et al* 1977) as a first-order approximation.

Table 1. Calculated ferromagnetic structure factors ($F(hkl)$) per unit cell of volume $(a_0)^3$, for $CeFe_2$.

(hkl)	$F(hkl)$
(111)	$8(f_{Ce}\bar{\mu}_{Ce}/\sqrt{2} - f_{Fe}\bar{\mu}_{Fe})$
(220)	$8f_{Ce}\bar{\mu}_{Ce}$
(311)	$8(f_{Ce}\bar{\mu}_{Ce}/\sqrt{2} + f_{Fe}\bar{\mu}_{Fe})$
(222)	$16f_{Fe}\bar{\mu}_{Fe}$

The ratio of measured/calculated ferromagnetic structure factors have been optimised according to the predictions of this table. The $Ce(Fe_{0.80}Co_{0.20})_2$ and $Ce(Fe_{1-x}Al_x)_2$ compounds have $\bar{\mu}_{Ce} = 0.0$, whereas $Ce(Fe_{1-x}Ru_x)_2$ with $x = 0.00$, 0.02 and 0.06 have $\bar{\mu}_{Ce}/\bar{\mu}_{Fe} = -0.3$, -0.3 and -0.35, respectively.

3.2.2. Antiferromagnetic Bragg scattering. The magnetic structure derived previously for antiferromagnetic $Ce(Fe_{1-x}Co_x)_2$ (Kennedy *et al* 1988) has been extended in this report, where we have included Cerium site contributions and non-centrosymmetric terms in the magnetic structure factor calculation, as well as a generalised expression for the spin orientation factor ($\bar{q}^2$) to include higher order antiferromagnetic reflections.

As before the antiferromagnetic structure factor for the Laves phase lattice $F_m(hkl)$ is expressed as a product of two terms

$$F_m(hkl) = F'_m(hkl)F''_m(hkl)$$

where $F'_m(hkl)$ is the magnetic structure factor for an FCC lattice and $F''_m(hkl)$ includes the interference terms from the six FCC basis points. For the first term ($F'_m(hkl)$) we consider the antiferromagnetic structure factor for an arrangement of spins with propagation vector $\tau = \langle 111 \rangle$ and average magnetic moment $\bar{\mu}$. The introduction of spin orientation lowers the lattice symmetry and requires doubling of the unit cell length ($a_m = 2a_0$). Thus the magnetic unit cell is expanded to $2 \times 2 \times 2$ FCC cells = 32 atoms, and

$$F'_m(hkl) = \begin{cases} 32f\bar{\mu} & \text{for } hkl \text{ all odd, such that } h+k,\ h+l,\ k+l = 4n+2 \\ 0 & \text{otherwise.} \end{cases}$$

where f is the magnetic form factor and (hkl) refers to the magnetic unit cell. Thus the multiplicity factor (j) of the allowed reflections is effectively reduced by 1/4. This antiferromagnetic structure is seen in the metal sites of the FCC 3d-metal oxides MnO, FeO, CoO and NiO (Roth 1958).

The atom positions for $F''_m(hkl)$ are Ce at $\langle \frac{3}{16}\frac{3}{16}\frac{3}{16} \rangle a_m$ and $\langle \frac{5}{16}\frac{5}{16}\frac{5}{16} \rangle a_m$ and Fe at $\langle 000 \rangle$, $\langle 0\frac{1}{8}\frac{1}{8} \rangle a_m$, $\langle \frac{1}{8}0\frac{1}{8} \rangle a_m$ and $\langle \frac{1}{8}\frac{1}{8}0 \rangle a_m$, where a_m is the magnetic cell length. The absence of the centre of symmetry requires consideration of both real and imaginary terms in the calculation of $F''_m(hkl)$. The resultant structure factor depends on the details of the antiferromagnetic spin arrangement, but for example in the simplest spin configuration with collinear moments involving only Fe sites we find reflections which satisfy $F'_m(hkl)$ give

$$|F''_m(hkl)|^2 = \begin{cases} 10 & \text{for } h = k = l \\ 2 & \text{otherwise.} \end{cases}$$

The difference between this calculation and the previous calculation where

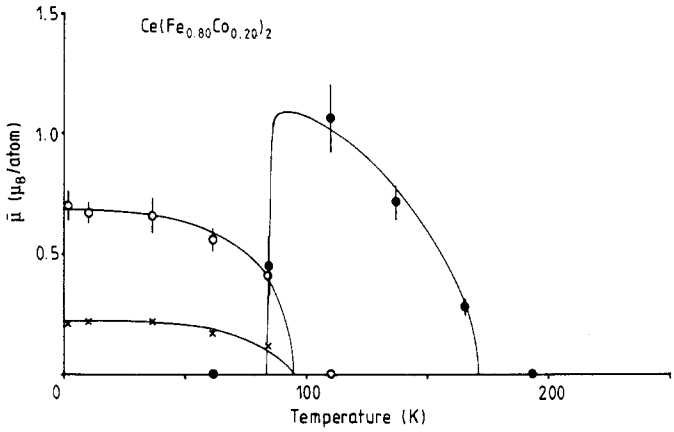

Figure 3. Temperature dependence of the ordered magnetic moment on the Fe sites in $Ce(Fe_{0.80}Co_{0.20})_2$. Ferromagnetic moment (●), antiferromagnetic moment (○) and lattice cell-axis angle (×).

$|F''_m(hkl)|^2 = 2$ for all reflections allowed by $F'_m(hkl)$ lies in the (hhh)-type reflections. Consequently, the calculated spin orientation angle (φ) for $Ce(Fe_{1-x}Co_x)_2$ in the previous report was incorrect.

A general expression for the average magnetic orientation term of the calculated antiferromagnetic Bragg scattering intensity for a powdered specimen is given by

$$\overline{q^2(hkl)} = [1 - \overline{(\hat{\boldsymbol{\rho}} \cdot \hat{\boldsymbol{\kappa}})^2}] \sin^2 \varphi + [1 - \overline{(\hat{\boldsymbol{\tau}} \cdot \hat{\boldsymbol{\kappa}})^2}] \cos^2 \varphi$$

where $\hat{\boldsymbol{\kappa}}$ is the unit scattering vector, $\hat{\boldsymbol{\tau}}$ is the unit antiferromagnetic propagation vector ($\tau = \langle 111 \rangle$), and $\hat{\boldsymbol{\rho}}$ is a unit vector perpendicular to τ ($\boldsymbol{\rho} = \langle 1\bar{1}0 \rangle$). The bar denotes the average over j, and φ is the angle between the magnetic moment vector (μ) and the antiferromagnetic propagation vector (τ) (note φ has been redefined to refer to the angle with respect to the propagation vector (τ) rather than with respect to the plane perpendicular to τ). Using this expression the analysis has been extended to include the first five antiferromagnetic reflections: (111). $(\bar{3}11)$, $(33\bar{1})$, (333, 511) and $(5\bar{3}1)$.

3.2.3. Magnetic results. The results of our magnetic analysis are summarised in the form of the magnetic phase diagrams presented in figures 2 to 5. The solid lines drawn through the data points have been included with consideration of the magnetic susceptibility measurements (χ_{AC}) of Rastogi and Murani (1987), and Roy and Coles (1987, 1988).

In the parent compound $CeFe_2$ (figure 2) we see the development of ordered moments on both Fe and Ce sites at T_c. These moments are coupled antiparallel such that $\bar{\mu}_{Ce}/\bar{\mu}_{Fe} = -0.3$. A small antiferromagnetic moment appears below $T \simeq 60$ K. The magnitude of this is too small for us to assess its temperature dependence accurately in these experiments, however by comparing the sum of antiferromagnetic diffraction intensities above and below 60 K the antiferromagnetic moment is estimated to be $\approx 0.15\ \mu_B$/Fe atom with an orientation $\varphi \approx 25°$ to τ.

Figure 3 shows the temperature dependence of the ordered moments in $Ce(Fe_{0.80}Co_{0.20})_2$. No ordered Ce moment is seen in either phase and the magnetic transition is a sharp one from ferromagnetism to antiferromagnetism, with $\varphi = 18.5°$.

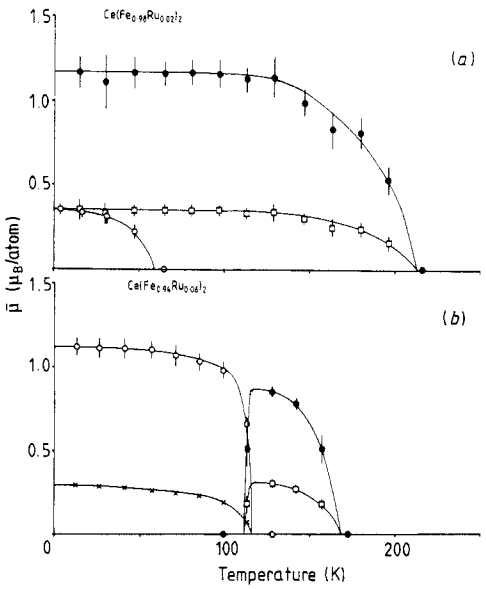

Figure 4. Temperature dependence of the ordered magnetic moment contributions in $Ce(Fe_{1-x}Ru_x)_2$, with (*a*) $x = 0.02$ and (*b*) $x = 0.06$. Ferromagnetic Fe-site moment (●), ferromagnetic Ce-site moment (□), antiferromagnetic moment (○) and lattice cell-axis angle (×).

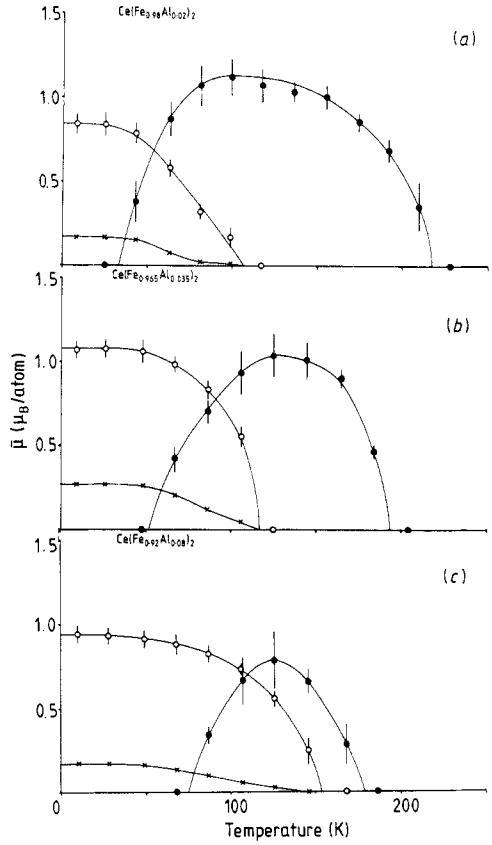

Figure 5. Temperature dependence of the ordered magnetic moment on the Fe sites in $Ce(Fe_{1-x}Al_x)_2$, with (*a*) $x = 0.02$, (*b*) $x = 0.035$ and (*c*) $x = 0.08$. Ferromagnetic moment (●), antiferromagnetic moment (○) and lattice cell-axis angle (×).

The rhombohedral lattice distortion at T_N is indicated by the change in cell axis angle ($\propto -90°$), which is indicated by crosses in the figure.

The compounds $Ce(Fe_{0.98}Ru_{0.02})_2$ and $Ce(Fe_{0.94}Ru_{0.06})_2$ (figures 4(*a*), (*b*)) show a progressive decrease of T_c with increasing Ru concentration, but with no obvious decrease in ferromagnetic moment magnitude. Here $\bar{\mu}_{Ce}/\bar{\mu}_{Fe} = -0.3$ and -0.35, respectively. The antiferromagnetic component ($\varphi = 18.5°$) is enhanced in $Ce(Fe_{0.98}Ru_{0.02})_2$ where a canted-spin phase exists below $T \simeq 60$ K, and in $Ce(Fe_{0.94}Ru_{0.06})_2$ antiferromagnetism exists on the Fe sites below $T_N \simeq 115$ K, with $\varphi = 18.5°$. In the latter compound, as in $Ce(Fe_{0.80}Co_{0.20})_2$, the apparent overlap between the magnetic phases is due only to the limited temperature resolution of these measurements. The rhombohedral lattice distortion at T_N in $Ce(Fe_{0.94}Ru_{0.06})_2$ is indicated by ($\varphi - 90°$) in figure 4(*b*) (crosses). No collinear cerium moment contributions to the antiferromagnetic phase could be detected.

The results for $Ce(Fe_{1-x}Al_x)_2$ with $x = 0.02, 0.035, 0.08$ are presented in figures 5(*a*), (*b*) and (*c*), respectively. No cerium moment contributions are seen in the ferromagnetic

phase. Ferromagnetic order occurs in all three compounds with a decrease in T_c with increasing Al concentration and a corresponding increase in the temperature at which the antiferromagnetic component appears. The antiferromagnetic components have $\varphi = 18.0°$, 18.0° and 19.0° to the ⟨111⟩ axis, respectively. The broad region of overlap between the two magnetic phases is the result of an extended region of canted spins. These results are in close agreement with the magnetisation measurements of Franceschini and da Cunha.

The characteristics of the lattice distortion in the M = Al compounds is also of interest. Although the lattice distorts with the appearance of antiferromagnetic components, its development is inhibited by the presence of a ferromagnetic component in the canted-spin phase, as indicated by the slow increase in α on cooling in figures 5(*a*), (*b*) and (*c*) (as compared with figure 3 and figure 4(*b*)). This observation is probably relevant to understand why the lattice remains cubic in $CeFe_2$ and $Ce(Fe_{0.98}Ru_{0.02})_2$ where antiferromagnetic components develop at low temperature but are considerably smaller than the ferromagnetic components.

4. Discussion

The temperature and concentration dependence of atomic cell volume for $Ce(Fe_{1-x}Ru_x)_2$ (figure 1) shows inflections at high temperature coresponding to a slight isotropic magnetostriction at the onset of ferromagnetic order, whereas the onset of an antiferromagnetic component is not reflected in the structure except for $Ce(Fe_{0.96}Ru_{0.04})_2$ where ferromagnetism disappears completely at the lower transition. Comparison with the earlier measurements on $Ce(Fe_{1-x}Co_x)_2$ shows the same structural response to antiferromagnetism (Kennedy *et al* 1988). The temperature dependence of the lattice distortion for $Ce(Fe_{0.96}Ru_{0.04})_2$ is qualitatively similar to $Ce(Fe_{0.80}Co_{0.20})_2$ and the low temperature values of $\alpha = 90.28°$ (Ru) and $\alpha = 90.20°$ (Co) are also comparable. Substitution of Ru results in an increase in lattice volume whereas substitution of Co results in a decrease in lattice volume, and it is interesting to note that either modification of the lattice enhances the instability of the ferromagnetism in $CeFe_2$.

Magnetic phase diagrams presented in figures 2 to 5 show the major differences between the magnetic properties of these pseudo binaries and give considerable insight into the magnetic character of $CeFe_2$. Substitution of Co provides a far more gradual decrease of T_c than Ru or Al, nor does ferromagnetism disappear entirely with large substitutions of Co (Rastogi and Murani, 1987). The former point may be related to the fact that the lattice volume decreases with Co substitution but increases with substitution of Al and Ru, and the latter point is perhaps not surprising if we regard alloys of $Ce(Fe, Co)_2$ with more than 50% Co as Fe substitution stabilising ferromagnetism in nearly ferromagnetic $CeCo_2$. However, the ferro-antiferromagnetic transition with Ru and Co substitutions are both quite sharp, whereas with M = Al the transition includes an extended overlap region.

The measurement of a low temperature canted spin phase in $CeFe_2$ as well as in the low concentration pseudobinaries shows that the tendency towards antiferromagnetic order is present in the parent compound itself and that the metallic substitutions simply enhance this tendency. The observation of an antiferromagnetic component at low temperature in $CeFe_2$ was recently verified in neutron diffraction measurements on single crystal $CeFe_2$ (Kennedy, Brown and Coles—to be published) where antiferromagnetic components developed below $T \simeq 80$ K.

The spin-canted phase of the M = Al compounds represents a continuous spin reorientation involving changing magnitudes of ferro and antiferromagnetic components, in which the spin orientation of the antiferromagnetic component is fixed at $\varphi \simeq 18.5°$ to the ⟨111⟩ axis. Whether the ferromagnetic spin orientation is fixed cannot be assessed here, but Atzmony and Dariel (1974) observed that the Fe moments of $CeFe_2$ are parallel to ⟨100⟩ between $T \simeq 80$ K and 150 K, and that above 150 K the moments cant towards ⟨111⟩ by ≃20°. However their report did not include measurements below 80 K. Pillay *et al* (1988) reported that in $Ce(Fe_{1-x}Co_x)_2$, with $x = 0.15$ and 0.25, Fe spins lie along ⟨100⟩ in the ferromagnetic phase but reorient towards ⟨111⟩ at T_N, and Nishihara *et al* (1987) reported Fe moments parallel to ⟨111⟩ in the antiferromagnetic phase and parallel to ⟨110⟩ in the ferromagnetic phase of $Ce(Fe_{0.95}Al_{0.05})_2$. With this information it is difficult to visualise how the two magnetic phases might coexist in a relatively simple total-spin configuration or how a transition between ferromagnetism and antiferromagnetism during spin reorientation may occur.

The figure for $Ce(Fe_{0.92}Al_{0.08})_2$ (figure 5(*c*)) clarifies the confusion over the interpretation of the spin glass like cusp in χ_{AC} (Roy and Coles 1989, Franceschini *et al* 1985). The figure indicates that the antiferromagnetic component begins to suppress the ferromagnetic response to external magnetic fields at a temperature quite close to T_c, so that for this compound the spin glass like cusp in χ_{AC} is really a reflection of the competing ferromagnetic and antiferromagnetic interactions. This effect may also explain why we see no decrease in the ferromagnetic moment at low temperature in $Ce(Fe_{0.98}Ru_{0.02})_2$ even though χ_{Ac} indicates a drop in ferromagnetic response below ≃ 20 K.

The magnetic structure of the antiferromagnetic component is largely as described previously (Kennedy *et al* 1988) except to note that the angle reported in this earlier report was incorrect due to the erroneous assumption that the antiferromagnetic structure is centrosymmetric. Using the correct analysis the average spin angle for the pseudobinaries in $\varphi = 18.4 \pm 0.3°$ to the ⟨111⟩ axis. This is the angle predicted for a collinear antiferromagnetic arrangement at the Fe sites with no Ce site contributions. It is also equivalent to the average orientation angle of a non-collinear multispin arrangement. The only high symmetry collinear spin direction close to this is ⟨112⟩($\varphi = 19.5°$). The possibility of multispin structures is not excluded by these results but we have been unable to find a multispin structure with cubic or rhombohedral symmetry which could provide antiferromagnetic structure factors compatible with those we have observed.

The only high symmetry non-collinear spin model which is close has Fe site spin directions of ⟨111⟩ at $\langle 000\rangle a_m$, ⟨110⟩ at $\langle \frac{1}{8}\,\frac{1}{8}\,0\rangle a_m$, ⟨1 0 1⟩ at $\langle \frac{1}{8}\,0\,\frac{1}{8}\rangle a_m$ and ⟨0 1 1⟩ at $\langle 0\,\frac{1}{8}\,\frac{1}{8}\rangle a_m$, but this yields $\varphi = 21°$ which is not within experimental error of the observed value. The inclusion of collinear Ce site moments modifies $F''_m(hkl)$ for $\bar{\mu}_{Ce}/\bar{\mu}_{Fe} = \pm 0.3$, but does not enhance the fit of calculated to measured structure factors.

The observation of ferrimagnetically coupled Ce moments in the ferromagnetic phase of $CeFe_2$ has recently been confirmed in our polarised neutron diffraction experiments on single crystal $CeFe_2$ (Kennedy *et al* 1990). Although we have assumed a 4f-electron-type form factor in our analysis of the Ce contributions in these materials, this cannot be considered proof that this is the correct form. Indeed Eriksson *et al* (1988) have suggested that Ce contributions in $CeFe_2$ would have dual 4f and 5d character, and such ferromagnetic A-site moments are strongly suggested for YFe_2 and $ZrFe_2$ where they must be of 4d character (Mohn and Schwartz 1985, Armitage *et al* 1986). However, the predictions of the two forms of magnetic scattering function are not sufficiently different over the measured range of $\sin\theta/\lambda \leqslant 0.23$ to influence the conclusions of this

work about the presence and orientation of the Ce moments. A detailed evaluation of the Ce form factor is outside the scope of these measurements but will be applied to our neutron diffraction results on single-crystal $CeFe_2$.

The presence of Ce contributions to the magnetic order in the ferromagnetic phase of $CeFe_2$ and $Ce(Fe_{1-x}Ru_x)_2$, but their absence in the antiferromagnetic phase raises the questions of what happens to these components at low temperature, and why the antiferromagnetic character of these compounds is not different from that of the pseudobinaries in which Ce moments are not present in the ferromagnetic phase? (It is also remarkable that we detect no ferrimagnetic Ce moment when as little as 2% Fe is replaced by Al). A feature of the D1B diffraction patterns of these compounds not discussed here is the appearance of low angle peaks below $T \simeq 150$ K in $CeFe_2$ and $Ce(Fe_{1-x}Ru_x)_2$. These peaks may be due to incommensurate ordering or magnetic short range order. Either way it seems likely that Ce site magnetic moments contribute to these peaks as they only appear in the compounds where we have observed ferrimagnetically aligned Ce moments. These peaks and the possible occurrence of magnetic diffuse scattering are the subject of further work currently under investigation.

Acknowledgments

Our thanks to Dr H E N Stone (IC) for sample preparation, R M Ibberson (RAL) for his assistance on HRPD, and Dr J K Cockcroft (ILL) for his assistance on D1B. This work was financially supported by the Neutron Beam committee of the SERC.

References

Armitage J G M, Dumelow T, Mitchell R H, Reidi P C, Abell J S, Mohn P and Schwartz K 1986 *J. Phys. F: Met. Phys.* **16** 1141–4

Atzmony U and Dariel M P 1974 *Phys. Rev.* **10** 2060–7

Eriksson O, Nordstrom L, Brooks M S S and Johansson B 1988 *Phys. Rev. Lett.* **60** 2523–26

Franceschini D F and da Cunha S F 1985 *J. Magn. Magn. Mater.* **52** 280–90

Freeman A J and Watson R E 1961 *Acta Crystallogr.* **14** 231–34

Johnson M W and David W I F 1985 *Rutherford Appleton Laboratory Report No* 85–112

Kennedy S J, Murani A P, Coles B R and Moze O 1988 *J. Phys. F: Met. Phys.* **18** 2499–2504

Kennedy S J, Brown P J and Coles B R 1990 to appear

Kennedy S J, Murani A P, Cockcroft J K, Roy S B and Coles B R 1989 *J. Phys. Condens. Matter* **1** 629–636

Lovesey S W 1986 *Theory of Neutron Scattering from Condensed Matter* vol 1 (Oxford: Oxford University Press) p 112

Mohn P and Schwartz K 1985 *Physica* **130** 26–8

Nishihara Y, Tokumoto M, Yamaguchi Y and Kido G 1987 *J. Magn. Magn. Mater.* **70** 173–4

Pillay R G, Grover A K, Balasubramanian V, Rastogi A K and Tandon P N 1988 *J. Phys. F: Met. Phys.* **18** 163–8

Rastogi A K and Murani A P 1987 *Proc. 5th Int. Conf. Valence Fluctuations (Bangalore)* (New York: Plenum)

Roth W L 1958 *Phys. Rev.* **110** 1333–41

Roy S B and Coles B R 1987 *J. Phys. F: Met. Phys.* **17** L215–20

—— 1988 *J. Appl. Phys.* **63** 4094–5

—— 1989 *J. Phys.: Condens. Matter* **1** 419–30

Roy S B, Kennedy S J and Coles B R 1988 *J. Physique Coll.* **49** C8 271–2

Stassis C, Deckman H W, Harmon B N, Desclaux J P and Freeman A J 1977 *Phys. Rev.* B **15** 369–76

Tandon P N, Pillay R G, Grover A K and Balasubramanian V 1989 *Hyperfine Interact.* **50** 733–40